

Infrared dispersion in SrTiO₃ at high temperature

J. L. Servoin,* Y. Luspain,[†] and F. Gervais

Centre de Recherches sur la Physique des Hautes Températures, Centre National de la Recherche Scientifique,
45045 Orléans Cedex, France

(Received 3 April 1980)

Infrared reflection spectra of strontium titanate are reported as obtained with a scanning interferometer from room temperature up to 1200 K. A fit of the factorized form of the dielectric function to reflectivity data yields the temperature dependence of TO and LO frequencies, dampings, and TO oscillator strengths. The soft TO mode is found to be coupled with the next TO mode. A significant deviation of the soft-mode behavior from the Curie law is evidenced above 400 K. The temperature dependence of the soft-mode damping is discussed.

I. INTRODUCTION

Two different theories^{1,2} were simultaneously presented to explain the hardening of the ferroelectric (FE) soft mode in strontium titanate. Chaves, Barreto, and Ribeiro¹ developed a theory based on a fourth-order anharmonic Hamiltonian which is restricted to a strong coupling between the soft optical mode and a transverse acoustic F_{1u} branch. Such a coupling had been evidenced by neutron scattering measurements.³ Earlier and in a more general way, Cowley⁴ evaluated *ab initio* the temperature dependence of transverse-optical (TO) and longitudinal-optical (LO) modes in SrTiO₃. This author found that the major anharmonic contribution which yields to the stabilization of the FE soft mode is that of the fourth-order anharmonic Hamiltonian at the lowest order. A similar theory for the mechanism of stabilization of a FE soft mode in the paraelectric (PE) phase of FE crystals was proposed by Silverman and Joseph.⁵ However, Migoni, Bilz, and Bäuerle² considered that an unrealistic fourth-order parameter had been used in Cowley's calculations, and showed that the behavior of the FE soft mode may be rather explained by the strongly anisotropic deformability of the oxygen ions. Both groups of authors^{1,2} fitted their model to the same set of experimental data obtained from liquid-helium temperature up to 400 K by neutron scattering,^{6,7} electric-field-induced Raman scattering,⁸ and infrared reflectivity measurements.⁹ All data points for the soft-mode frequency squared are approximately aligned and nearly obey a law of the form

$$\Omega_s^2 = A(T - T_c) \quad (1)$$

above 50 K, with T_c near 32 K.¹ Deviations from this law at low temperature, understood in term of

zero-point lattice fluctuations, were correctly fitted by both models.^{1,2} However, while the fourth-order anharmonicity^{1,4} yields a straight line according to Eq. (1) above the Debye temperature, Migoni *et al.*² found that the quantity A of Eq. (1) slightly decreases with increasing temperature. One of the purposes of the present study was to obtain experimental data at higher temperatures to see whether the deviation from the law Eq. (1) is important or not, owing to the consequences that such a deviation would imply concerning the mechanism of the ferroelectricity. We have, therefore, performed infrared reflectivity measurements as a function of temperature via a new technique—Fourier transform scanning interferometry—which we have developed recently¹⁰ to study other FE materials such as LiTaO₃, LiNbO₃, BaTiO₃, and KNbO₃.

II. INFRARED REFLECTION SPECTRA

Experimental conditions were detailed in Refs. 10 and 11. The temperature dependence of infrared reflectivity of strontium titanate, as obtained with a Bruker IFS 113C scanning interferometer, is shown in Fig. 1 from room temperature up to 1200 K. The infrared reflection measured at room temperature agrees reasonably well with previous measurements.¹² The evolution of the TO mode structure on heating is displayed in Fig. 2 as obtained from a Kramers-Kronig analysis of reflectivity data. The classical dispersion theory is unable to fit the spectra of oxidic perovskites.¹²

For such wide band spectra, a model based on the factorized form of the dielectric function

$$\epsilon = \epsilon_\infty \prod_j \frac{\Omega_{jLO}^2 - \omega^2 + i\gamma_{jLO}\omega}{\Omega_{jTO}^2 - \omega^2 + i\gamma_{jTO}\omega} \quad (2)$$

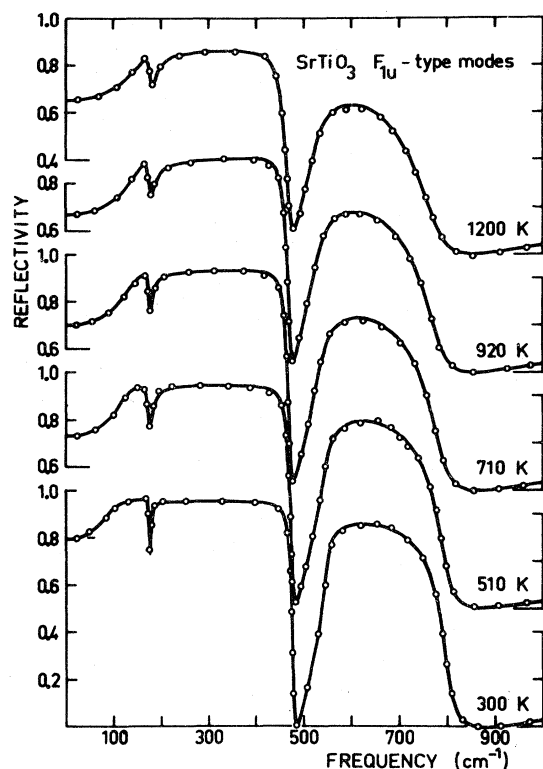


FIG. 1. Infrared reflection spectra as a function of temperature. Curves are the best fit to the model Eq. (2) to experimental data.

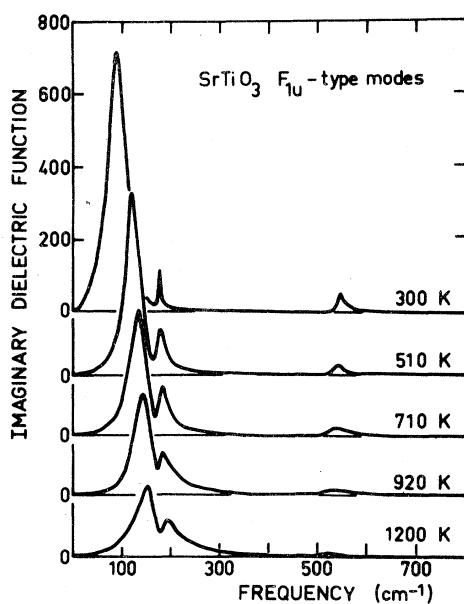


FIG. 2. Temperature dependence of the imaginary part of the dielectric function as obtained from a Kramers-Kronig analysis.

where Ω_{JTO} , Ω_{JLO} , and γ_{JLO} represent frequencies and dampings of TO and LO modes, respectively, first employed by Berreman and Unterwald¹³ and developed to incorporate phonon self-energy effects after some simplifying assumptions,¹⁴⁻¹⁶ has been successfully used to fit infrared reflection spectra of crystals such as corundum Al_2O_3 ,¹⁴ rutile,¹⁷ and reduced rutile^{18,19} (taking account of LO phonon-plasmon coupling). Justification for this product form, therefore, will not be stated here again. More interesting is to recall that infrared reflection spectra of BaTiO_3 we had obtained at room temperature were compared to Raman data,²⁰ because A_1 - and E -type modes are both infrared and Raman active in the tetragonal FE phase. It was shown that TO and LO Raman peaks and linewidths entered in the factorized form of the dielectric function Eq. (2) readily yield the experimental infrared reflectivity. Merely, some minor refinements of the parameters were necessary to get the best fit.²⁰ It seems therefore there is no need to invoke off-diagonal coupling terms in the phonon response matrix²¹ to describe such spectra. Besides, excellent fits to BaTiO_3 spectra obtained in the range 300–1400 K were reported recently and coupling between the soft mode and the next TO mode was confirmed to be very small.²²

Figure 1 shows that the model Eq. (2) again is successful in fitting accurately infrared reflection spectra of strontium titanate at all temperatures. Figure 3 shows an example of agreement between the dielectric function which yields the best fit to reflectivity data and that evaluated from a Kramers-Kronig analysis. Transmission measurements were also performed as a function of temperature and confirmed the experimental results of Ref. 23.

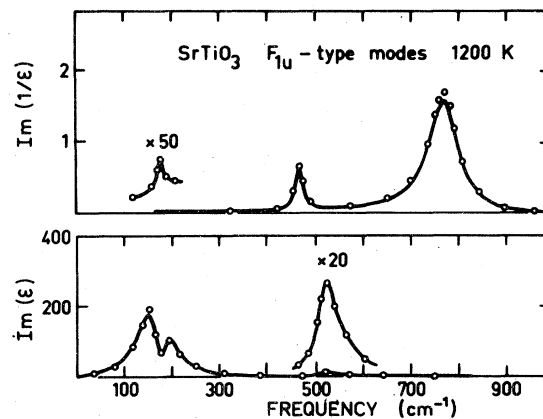


FIG. 3. Comparison between Kramers-Kronig analysis (dots) and the dielectric function Eq. (2) which fits reflectivity data.

III. ANALYSIS OF THE DATA

A. Frequencies

The temperature dependence of TO and LO frequencies deduced from the best fit to reflectivity data is plotted in Fig. 4. Mode frequencies above 400 cm⁻¹ decrease smoothly with increasing temperature, as commonly observed. Data for the soft-TO-mode frequency agree with those reported previously at temperatures lower than 400 K.⁶⁻⁸ The square of the frequency of the lowest-energy modes is plotted in

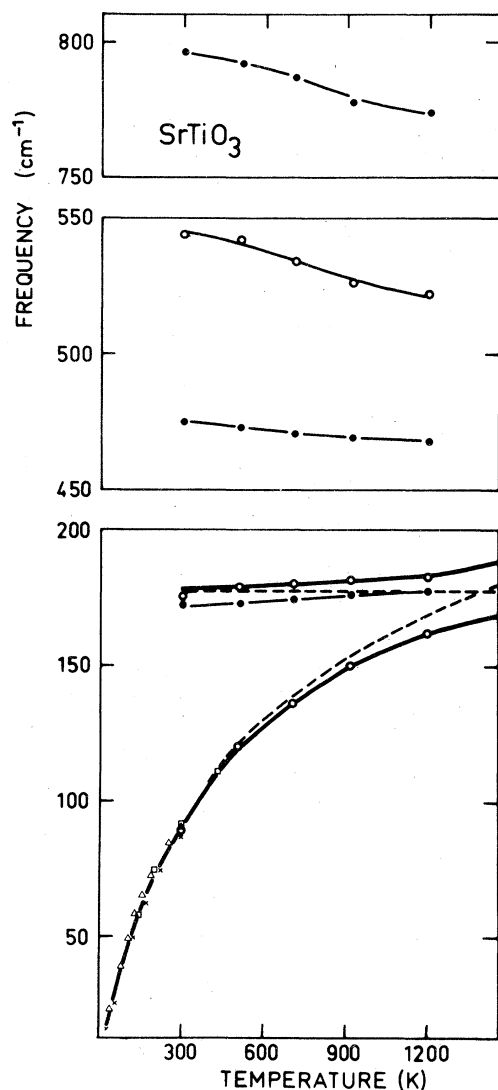


FIG. 4. Temperature dependence of optical frequencies. Open and full circles are present TO- and LO-mode frequencies. Other symbols are results taken from Refs. 6-8. Heavy lines in the lower part of the figure represent a fit of the model Eq. (3) to the data. Dashed lines are decoupled-mode frequencies. Small lines are guide to eyes.

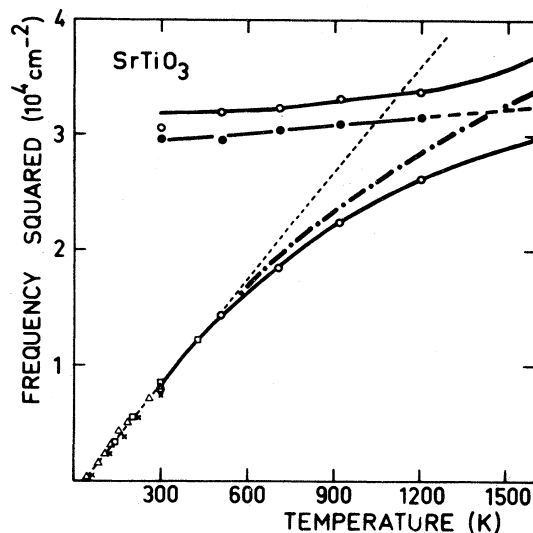


FIG. 5. Temperature dependence of the square of frequencies. The dashed line is an extrapolation of the Curie law up to high temperature. The dash-dot curve is the decoupled-soft-mode frequency squared. Same as legend to Fig. 4 for other symbols.

Fig. 5. An important deviation from the linear law is found at high temperature. However, since the soft mode nearly reaches the next polar mode and the latter also increases with increasing temperature contrary to modes of higher energy, there are indications of coupling between both modes. We have decoupled the system of both TO modes with the very simple formula²⁴

$$\Omega_{\pm} = \frac{1}{2}(\omega_1 + \omega_2) \pm \frac{1}{2}[(\omega_1 - \omega_2)^2 + 4w^2]^{1/2}, \quad (3)$$

where Ω_+ and Ω_- represent the experimental coupled-mode frequencies shown in Fig. 4. After making the approximation that the uncoupled-mode frequency at 177 cm⁻¹ is temperature independent, then good fit to Ω_+ and Ω_- data can be achieved with the weak-coupling constant $w = 10$ cm⁻¹ and the decoupled-soft-mode frequency shown by a dashed curve in Fig. 4. The significant deviation of the decoupled-soft-mode frequency squared from the linear regime above 500 K is thus unambiguously confirmed as shown in Fig. 5. This important result will be discussed in the last section.

B. Oscillator strengths

The strengths of the three polar oscillators are deduced from the TO-LO splittings with the formula

$$\Delta\epsilon_j = \epsilon_{\infty} \frac{\Omega_{jLO}^2 - \Omega_{jTO}^2}{\Omega_{jTO}^2} \prod_{k \neq j} \frac{\Omega_{kLO}^2 - \Omega_{jTO}^2}{\Omega_{kTO}^2 - \Omega_{jTO}^2}. \quad (4)$$

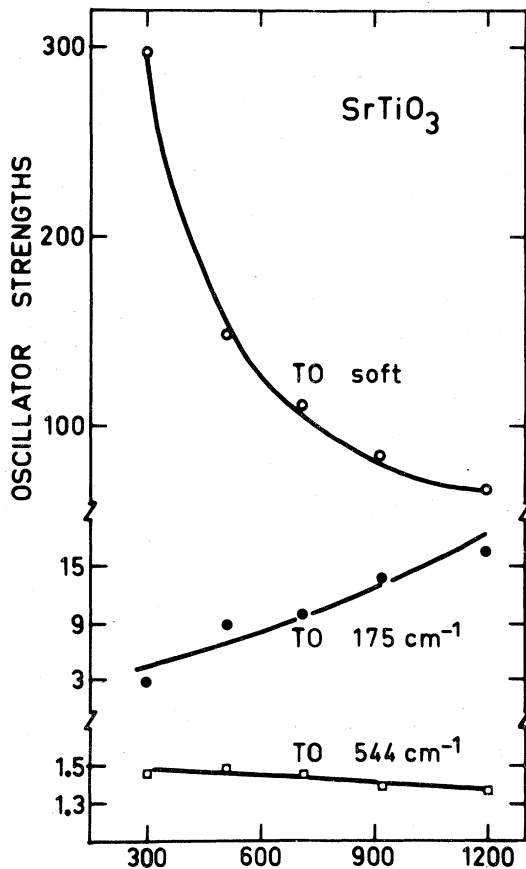


FIG. 6. Temperature dependence of TO oscillator strengths.

Results are plotted in Fig. 6. It is clear that the soft-mode oscillator strength carries nearly all the contribution to the static dielectric constant and decreases on heating roughly according to the Curie law. At the highest temperatures however there is a beginning of intensity transfer with the next TO mode, consistent with the coupling phenomenon. Let us recall that the static dielectric constant^{25,26} agrees with our result $\epsilon(0)$ as calculated with Eq. (2), or equally to $\epsilon_\infty + \sum_j \Delta\epsilon_j$ at all temperatures within experimental error.

C. Damping

The temperature dependence of the soft-TO-mode damping is shown in Fig. 7 and that of all other modes in Fig. 8. We will merely follow an approach which was shown to be successful for the description of the temperature dependence of phonon lifetimes in crystals which do not undergo structural phase

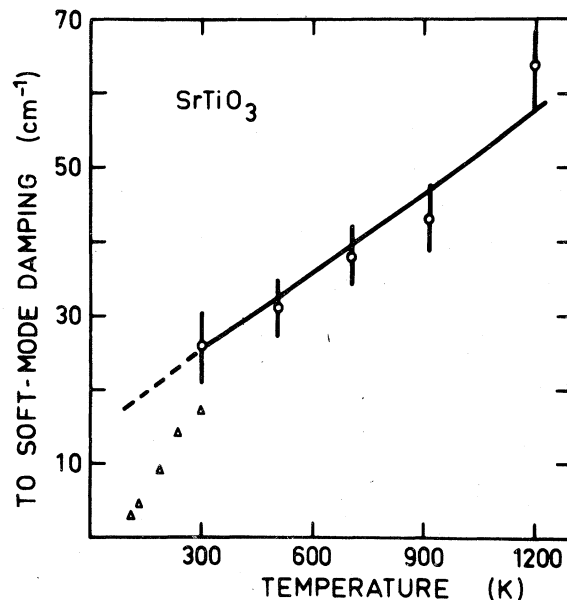


FIG. 7. Dependence of the soft-mode damping vs temperature. Triangles are Raman linewidths (Ref. 8). Circles are present data. The curve is an attempt of fit of the model Eq. (5) to damping data above room temperature.

transformations. The following model

$$\gamma_j(T) = \gamma_j(0) \left\{ n \left[\frac{1}{2} \Omega_j(T) \right] + \frac{1}{2} \right\}, \quad (5)$$

where

$$n(\omega) = \exp[(h\omega/k_B T) - 1]^{-1} \quad (6)$$

is the mean number of phonons, was shown to explain satisfactorily the temperature dependence of any damping constant in common oxide crystals.^{14,17} The model Eq. (5) is deduced from the imaginary part of the phonon self-energy function²⁷ after some simplifying assumptions. Cubic additive anharmonic processes only are retained and the fact that the frequencies in the combinations of two phonons which relax the j th phonon are dispersed on both sides of the frequency $\frac{1}{2}\Omega_j$ to satisfy the energy conservation law is merely taken into account. As might be expected on the other hand, this very simple model was shown to be inadequate to fit the temperature dependence of phonon linewidths near structural phase transitions in crystals like quartz²⁸ and lead phosphate.²⁹ Fits of the model Eq. (5) to experimental data are shown in Fig. 8. Such a result indicates that in strontium titanate all mode but the soft-mode lifetimes behave "normally."

Fleury and Worlock⁸ focused attention on the fact that their soft-mode Raman linewidths are very different from infrared dampings.³⁰ At 85 K, for exam-

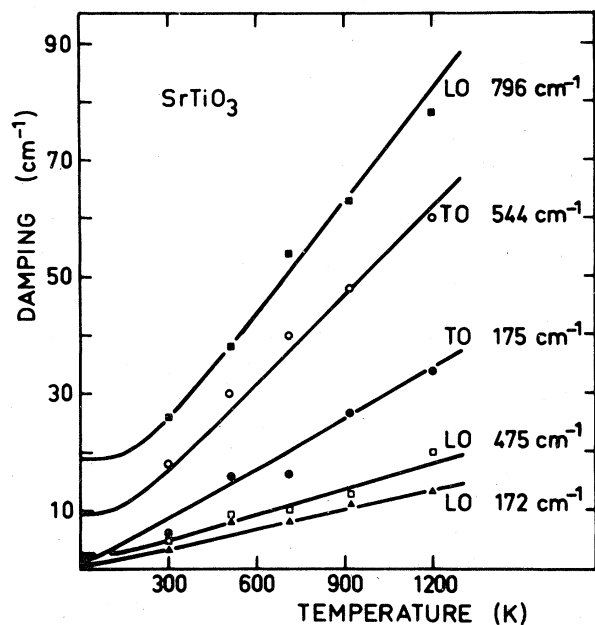


FIG. 8. Temperature dependence of damping (dots). Full lines are fit of the model Eq. (5) to the data.

ple, the Raman damping is found some 20 times smaller than the infrared value. At room temperature, our infrared damping is found to be 27 cm^{-1} whereas the Raman linewidth is only 17 cm^{-1} .⁸ It could be thought that the higher value found from our infrared reflectivity experiment is due to the small penetration depth of the infrared radiation in SrTiO₃ near the soft-mode resonance. The absorption coefficient indeed reaches the value $\sim 40\,000 \text{ cm}^{-1}$ which yields a penetration depth much shorter than $1 \mu\text{m}$. Then a disorder induced by surface polishing could significantly increase the soft-mode damping although we had taken the precaution to anneal the crystal at high temperature to regenerate the surface altered by the polishing. The contribution of surface disorder to the linewidth may be estimated to be temperature independent. On the basis of the data of Ref. 8, one could thus consider that the soft-mode linewidth in the bulk would be some 10 cm^{-1} lower than values found from surface measurements. This is significant at room temperature and below, but the discrepancy is only 15% at 1200 K, that is near the usual experimental inaccuracy. It should be emphasized however that in recent results in SrTiO₃ at room temperature obtained by hyper-Raman scattering,³¹ 24 cm^{-1} is reported for the soft-mode damping, thus in close agreement with our value. More generally, our TO- and LO-mode linewidths and frequencies agree with the data of Ref. 31 obtained from measurements in the bulk.

It could be thought that coupling with the TO

mode at 175 cm^{-1} would yield a transfer of damping between both modes, as well as for the oscillator strengths (Fig. 6). It seems however that this effect is still weak at 1200 K since the temperature dependence of TO- 175-cm^{-1} - and LO- 172-cm^{-1} -mode dampings do not display any anomaly at high temperature (Fig. 8). This is likely so because both uncoupled modes have not yet crossed each other at 1200 K (Fig. 4). Let us merely note in passing that the model Eq. (5) is also able to fit the temperature dependence of present soft-mode infrared damping reasonably well. In this temperature range, the soft-mode frequency increases from 89 up to 162 cm^{-1} . But, as might be expected, the model becomes inadequate if the phonon decay channels are completely modified when the mode shifts up considerably as it is the case in strontium titanate. Thus, irrespective of the possible systematic "errors" due to surface alterations and mode coupling—taking account of the fact that both effects would lower the observed damping—the unambiguous change of slope of the soft-mode damping profile on increasing temperature is ascribed to changes of phonon decay channels consistent with the fact that the phonon energy is increased by a factor 3.3 from 110 up to 1200 K.

IV. DISCUSSION

The behavior shown in Fig. 4 indicates that the soft-mode frequency does not increase indefinitely but rather would tend towards a frequency which constitutes the limit of stability. We thus confirm the hypothesis put forward to explain the behavior of the static dielectric constant at high temperature which was fitted to a modified Curie-Weiss law.²⁵

We would like to discuss the results of the calculations of Cowley⁴ which predict the temperature dependence of TO and LO phonon frequencies and their linewidths from 100 to 400 K. It was found that *all frequencies* increase with increasing temperature. If this behavior is experimentally verified for the two lowest-frequency TO modes and the intermediate LO mode—although less marked for the modes at 172 and 175 cm^{-1} than predicted theoretically—a marked decrease of the three other mode frequencies is observed contrary to theoretical predictions. Therefore, since the only positive contribution to the real part of the phonon self-energy (which causes the frequency shift) is the lowest-order fourth-order anharmonicity, it seems that a too large fourth-order parameter had been used in Cowley's calculations, as emphasized by Migoni *et al.*² But if this parameter is reduced to account for the temperature dependence of high-frequency modes, then fourth-order anharmonicity alone becomes insufficient to explain the stabilization of the soft mode

within Cowley's model approximation. Of course, higher-order anharmonic interactions could be invoked to explain the deviation from the linear law. Such contributions, which were not taken into account in the calculations of Refs. 1 and 4 indeed yield a temperature dependence of the form T^α with $\alpha \geq 2$ above the Debye temperature. Most of them have a negative sign. But the problem that the fourth-order anharmonic parameter should be *further increased* in order that the addition of negative higher-order terms would yield a resulting profile which would fit experimental data remains raised. On the other hand, present experimental results seem to support the oth-

er theory based on the strong anisotropy of the oxygen polarizability as proposed by Migoni *et al.*²

ACKNOWLEDGMENTS

The sample grown by K. Bethe at the Rheinisch-Westfälischen Technischen Hochschule, Aachen, has been kindly supplied by B. Jannot. Numerical calculations have been performed with the CII 10070 computer of the Centre Interuniversitaire de Calcul de la Région Centre, Orléans.

*U.E.R. Sciences Fondamentales et Appliquées, Université d'Orléans, France.

†Permanent address: Laboratoire d'Etudes Physiques des Matériaux, E.R.A. No. 13, Université d'Orléans, 45045 Orléans Cedex, France.

¹A. S. Chaves, F. C. S. Barreto, and L. A. A. Ribeiro, *Phys. Rev. Lett.* **37**, 618 (1976).

²R. Migoni, H. Bilz, and D. Bäuerle, *Phys. Rev. Lett.* **37**, 1155 (1976).

³J. D. Axe, J. Harada, and G. Shirane, *Phys. Rev. B* **1**, 1227 (1970).

⁴R. A. Cowley, *Philos. Mag.* **11**, 673 (1965).

⁵B. D. Silverman and R. S. Joseph, *Phys. Rev.* **129**, 2062 (1963).

⁶R. A. Cowley, *Phys. Rev.* **134**, A981 (1964).

⁷Y. Yamada and G. Shirane, *J. Phys. Soc. Jpn.* **26**, 396 (1969).

⁸P. A. Fleury and J. M. Worlock, *Phys. Rev.* **174**, 613 (1968).

⁹A. S. Barker and M. Tinkham, *Phys. Rev.* **125**, 1527 (1962).

¹⁰F. Gervais, Y. Luspin, J. L. Servoin, and A. M. Quittet, *Ferroelectrics* **24**, 285 (1980).

¹¹F. Gervais and J. L. Servoin, *Infrared Phys.* **18**, 883 (1978).

¹²W. G. Spitzer, R. C. Miller, D. A. Kleinman, and L. E. Howarth, *Phys. Rev.* **126**, 1710 (1962).

¹³D. W. Berreman and F. C. Unterwald, *Phys. Rev.* **174**, 791 (1968).

¹⁴F. Gervais and B. Piriou, *J. Phys. C* **7**, 2374 (1974).

¹⁵F. Gervais and J. L. Servoin, *Phys. Rev. B* **15**, 4532 (1977).

¹⁶J. L. Servoin and F. Gervais, *Appl. Opt.* **16**, 2952 (1977).

¹⁷F. Gervais and B. Piriou, *Phys. Rev. B* **10**, 1642 (1974).

¹⁸F. Gervais and J. F. Baumard, *Solid State Commun.* **21**, 861 (1977).

¹⁹J. F. Baumard and F. Gervais, *Phys. Rev. B* **15**, 2316 (1977).

²⁰J. L. Servoin, F. Gervais, A. M. Quittet, and Y. Luspin, *Phys. Rev. B* **21**, 2038 (1980).

²¹A. S. Barker and J. J. Hopfield, *Phys. Rev.* **135**, A1732 (1964).

²²Y. Luspin, J. L. Servoin, and F. Gervais, *J. Phys. C* **13**, 3761 (1980).

²³P. Rochon, J. L. Brebner, and D. Matz, *Solid State Commun.* **29**, 63 (1979).

²⁴J. F. Scott, *Rev. Mod. Phys.* **46**, 83 (1974).

²⁵G. Rupprecht and R. O. Bell, *Phys. Rev.* **135**, A748 (1964).

²⁶G. A. Samara, *Phys. Rev.* **151**, 378 (1966).

²⁷A. A. Maradudin and A. E. Fein, *Phys. Rev.* **128**, 2589 (1962).

²⁸F. Gervais, *Ferroelectrics* **13**, 555 (1976).

²⁹Y. Luspin, J. L. Servoin, and F. Gervais, *J. Phys. Chem. Solids* **40**, 661 (1978).

³⁰A. S. Barker, *Phys. Rev.* **145**, 391 (1966).

³¹H. Vogt and G. Neumann, *Phys. Status Solidi (b)* **97**, 57 (1979).